Photo-electrochemical and Photo-catalytic Conversion of Carbon Dioxide

York R. Smith,[1, 2] Vaidyanathan (Ravi) Subramanian,[2] and B. Viswanathan[1*]

[1]National Centre for Catalysis Research,

Indian Institute of Technology-Madras, Chennai 600 036, India

[2]Chemical & Materials Engineering Department, University of Nevada, Reno 89557 USA

[*] To whom correspondence should be addressed:
E-mail: bvnathan@iitm.ac.in
Ph: 091-44-2257424; Fax: 091-44-22574202

Abstract

The conversion of carbon dioxide to useful chemicals has been the subject of numerous investigations. Though there are a variety of activating methods, only electrochemical and photo-electrochemical activation of carbon dioxide have shown promise till date. However in this area, the extent of conversion and also the evolution of method for a specific chemical from carbon dioxide appear to be a far dream. The present article deals with a critical evaluation of knowledge available in literature in this important area.

1. Introduction

Increasing emissions levels from combustion of fossil fuels in stationary and mobile energy conversion systems, as well as emissions from various industrial processes, have raised many environmental and health concerns in recent years. These emissions into the atmosphere include pollutants such as NO_X, SO_X, particulate matter, and greenhouse gases (GHG) such as methane (CH_4), chlorofluorohydrocarbons (CFCs), and carbon dioxide (CO_2). Succinctly, anthropogenic GHG emissions into the atmosphere have been speculated to play a role in global climate change[1] and have sparked multiple initiatives to reduce such emissions, with particular emphasis on CO_2.[1-3]

The sources of CO_2 emissions include stationary, mobile, and natural as listed in Table 1. Anthropogenic emissions include those from energy utilization from mobile and stationary

sources, but exclude natural sources. Figure 1 displays the change in the global atmospheric CO_2 concentration over the millennium from 1000-2004 based on recent studies of Antarctic ice core samples.[4] The estimated CO_2 concentration in the atmosphere remained steady at 280 ppmv (parts per million by volume) for the majority of the millennium, but increased to 315 ppmv in 1958 (US Industrial Revolution) and further to 377 ppmv in 2004 based on actual analysis conducted in Hawaii, USA.[5] Current estimations state that the atmospheric CO_2 concentration is around 384 ppmv and is forecasted to increase at a rate of approximately 1% per annum. Such increases in atmospheric CO_2 are primarily caused by the combustion of fossil fuels for energy consumption (25%) and deforestation (10-30%).[3] However, it should be mentioned that although CO_2 and other GHG's are suspected to play a role in global climate change, atmospheric CO_2 has an important and positive role in the ecological system, since photosynthesis and food production depend on it as a carbon source. Furthermore, fossil fuels used today originated from atmospheric CO_2 millions of years ago. Nevertheless, the research conducted in the last five decades, and more notably the last 15 years, shows drastic increase in CO_2 emissions in the last century with a continuing increase at much faster rates than previous years (Figure 2). As a result of the potential adverse effects of high CO_2 atmospheric concentrations to humans and the environment, a large effort has been put forth to reduce CO_2 emissions from major contributing sources. Methods for CO_2 mitigation can be achieved by the following:

- CO_2 sequestration;
- Post-treatment capture and utilization (recycle);
- Increase in efficiencies of carbon-based energy systems;
- Use of carbon-free alternative energy sources;

When examining methods for CO_2 mitigation, the process should be efficient and should not require substantial energy input from conventional energy systems (e.g. fossil fuel power generation). Sequestration of CO_2 in geological formations such as deep-sea beds or use in enhancing fossil fuel recovery is a highly debated method. The ability for such systems to handle billions of tons per year is still unanswered. Moreover, the processes for sequestration requires large energy input, which in turn leads to more GHG emissions if supplied by conventional power generation methods. The increase in efficiencies of carbon-based energy systems will help reduce future emissions; however, it does not supply an avenue to reduce existing CO_2 atmospheric concentrations. On the other hand, implementing carbon-free alternative energy sources requires significant socio-economic changes. These methods raise many political, environmental, and economic concerns. Conversely, converting or recycling CO_2 into value-added products, such as high-energy content fuels suitable for utilization in existing infrastructure appears to be an attractive option.

Conversion of CO_2 into value added products could be achieved in a number of ways. A review by Xiaoding and Moulijn[3] covers many catalytic conversion processes of CO_2. Reactions involving CO_2 can be, to some extent, energy input intensive. Thus, the energy required for the conversion process should come from processes that do not emit more GHGs directly into the atmosphere. When evaluating the current technologies available for the storage and conversion of CO_2, they do not fall within these criteria.

One avenue that has been extensively studied to convert CO_2 is through electrochemical reduction.[6,7] Several studies have reported converting CO_2 into various forms such as carbon monoxide,[8] formaldehyde, formic acid,[9] methanol,[10] ethanol,[11] n-propanol,[12] methane,[8] ethane, and ethylene.[13] Although several reports indicate high Faradaic efficiencies (~95%) with

electrochemical reduction of CO_2 to such fuels, there are still limitations within such systems, mainly owning to:

- kinetic limitations due to low solubility of CO_2 in water;
- competition with hydrogen evolution reaction in aqueous solutions;
- high-energy demand for conversion;
- uncontrolled intermediates.

In order to develop a process that is not only *green* but also is able to address some of the aforementioned limitations, the energy required for the reduction process preferably should be supplied by renewable and/or alternative sources. One such avenue, which still requires a more in-depth study, is the photo-electrochemical and photo-catalytic reduction of CO_2 to simple alcohols and low chain hydrocarbon fuels. Photo-electrochemical and photo-catalytic reduction of CO_2 are very similar in that a large portion (photo-electrochemical) to all (photo-catalytic) the energy required for the reduction is supplied by solar irradiation rather then external source (e.g., fossil fuel power plant).

The photo-catalytic activation and reduction of CO_2 has been attempted in a number of ways using suitable catalysts, sensitizers, transfer and sacrificial agents in both homogeneous and heterogeneous systems.[14] These recent studies have introduced the photo-reduction of CO_2 as a potential application to convert to fuels such as methane, methanol, ethanol, and formic acid. An important feature of the photo-electrochemical reduction of CO_2 is not only the utilization of process-waste CO_2 streams as a fuel source, but such systems utilize the most abundant sources of energy and hydrogen, being sunlight and water, respectively. Solar photo-electrochemical and photo-catalytic reduction to produce fuels by use of water as the hydrogen source thus has the potential to be a means to store intermittent solar energy and recycle CO_2 while decreasing the

use of fossil fuels, and in turn harmful GHG emissions. Despite recent advancements in the field of photo electrochemistry and photo-catalysis with regard to CO_2 conversion, yields are quite low and still warrant a comprehensive investigation.

1.1 Photo electrochemistry (PEC) and Photo catalysis

Ever since the discovery of the photoelectric effects of two metal electrodes immersed in a conducting medium by the French scientist Edmond Becquerel,[15] researchers and engineers have been probing the idea of converting light energy into electrical power and chemical fuels. Several advances between the years of 1955 and 1971 improved the understanding of electrochemical interactions between semiconductor-liquid interfaces, namely by Gerischer, Memming, and Williams, among others (and references there within).[16-18] Although such applications of solar light energy conversion were considered early on, Fujishima and Honda[19] first demonstrated the realization of such systems with the photo electrolysis of water to hydrogen and oxygen at a semiconductor electrode (TiO_2). Subsequently, several review articles extensively cover the advancements of PEC and photo-catalysts over the years for several applications from wastewater remediation to hydrogen production and CO_2 photoreduction.[14,20-26]

Figure 3 shows a schematic of a liquid-junction photo-electrochemical cell. It consists of a photoanode, a counter electrode cathode, and a reference electrode. In a typical PEC setup, semiconductors utilize light irradiation to promote reactions on the surface of the electrodes within the system. For this example we will consider n-type semiconductors, since they have generally shown better stability. The principles and applications of p-type materials are generally similar to n-type materials. Oxidation of the electrolyte (e.g., H_2O) occurs at the anode and reduction occurs at the cathode.

An innate property that makes semiconductors useful for PEC is their discrete quantum states of electrons. Unlike their metal counterparts that have a continuum of electron states (bands), semiconductors exhibit an electrical resistivity, or rather an energy band gap (E_g) that extends from the top of the filled valance energy band (VB) to the bottom of the vacant conduction energy band (CB). In general, when a semiconductor surface is exposed to light radiation ($h\nu \geq E_g$) electron hole pairs ($e_{CB}^- - h_{VB}^+$) are generated, represented by eqn 1 with heat generation for the reverse reaction as shown by eqn 2.

$$photocatalyst \xrightarrow{h\nu \geq E_g} \left(h_{VB}^+ + e_{CB}^-\right) \quad (1)$$

$$photocatalyst + \left(h_{VB}^+ + e_{CB}^-\right) \rightarrow heat \quad (2)$$

Upon photo-excitation of an electron from the VB to the CB, the e_{CB}^- and h_{VB}^+ pairs can follow several pathways. Ideally, in a PEC cell the photo-generated e_{CB}^-'s are driven to the external circuit and subsequently to the cathode with a small bias potential. The h_{VB}^+'s can then migrate to the surface of the semiconductor to oxidize any absorbed molecules or solvent on the surface. The ability for a photo-catalyst to carry out redox reactions and facilitate effective and efficient charge transfer is predisposed to efficient charge separation and its ability to absorb reacting species on the photo-catalyst surface. Although the lifetime of the ($e_{CB}^- - h_{VB}^+$) pairs are on the order of 10^{-15}~10^{-12} seconds,[27-29] it is still sufficient to promote redox reactions on the surface of the respective electrodes. At the surface of the semiconductor, electrons can also be donated to an acceptor species and likewise the holes can migrate to the surface to combine with electrons from a donor species as well. However, the recombination of electrons and holes prevents them

from transferring to the surface to react with absorbed species and likewise can occur within the volume of the semiconductor or on the surface of the semiconductor. The rate at which charge transfer occurs depends up the position of the bands and the redox potential of the absorbed species of interest. For the activation and photo-reduction of CO_2, this concept plays a significant role (*vide infra*).

For photo-catalytic systems, Bard's concept[20] can be applied. This suggests that semiconductor particles, or powders themselves can act as a short-circuited PEC by providing both oxidizing and reducing sites for the reaction (Figure 3b). When comparing the two systems, the photo-catalytic system is simpler and easy to construct. As a result, some important factors that should be met for optimal performance of a photo-catalytic process include the following:

- The redox potential of the photo-generated VB hole should be sufficiently positive for the hole to act as an acceptor;
- The redox potential of the photogenerated CB electron should be sufficiently negative for the electron to act as a donor;
- Photocatayst should be economically available and be environmentally inert;
- Photo-catalyst should be stable (Photo-stable) in a wide pH range and in a variety of electrolytes.

For the photo-reduction of CO_2, large band-gap semiconductors are more suitable as they provide sufficient negative and positive potential in conductance and valance bands, respectively. However, the disadvantage of using wide band gap semiconductors is the high-energy input requirement and thus a limitation of a small portion of the solar spectrum. For example, titania (TiO_2) is a widely studied and stable photo-catalyst with a large band gap (~3.2 eV for anatase), is active in the ultraviolet (UV) region of the solar spectrum which only

constitutes ~3-6% of the solar spectrum. Although a semiconductor such as cadmium sulfide (CdS) has a smaller band gap (~2.25 eV) and is visible-light active (~46-50% of the solar spectrum), its VB is not sufficiently positive enough to act as an acceptor and thus causes the photocatlayst to corrode[30]. Despite decades of work with TiO_2 to improve its properties via doping and addition of other photoactive materials, results have only demonstrated incremental improvements in photo-catalytic performance.[31,32] Thus, a material with a valance band that is sufficiently positive, a conduction band that is sufficiently negative to promote smooth electron transfer of absorbed CO_2 molecules, and is visible-light active would be the ideal material for the photo-reduction of CO_2.

2. Photo-reduction of CO_2

2.1 Survey on the photo-electrochemical & photo-catalytic reduction of CO_2

The photo-electrochemical and photo-catalytic reduction of CO_2 on semiconductor electrodes has gained much attention in recent years. Studies have been extended to a variety of different avenues such as analysis of various semiconductor photocatalysts,[33-36] modification of photo-catalyst by depositing small amounts of metal[37,38] and metal complexes,[39,40] and the effects of operating conditions.[41-43] In general, the photo-electrochemical and photo-catalytic reduction of CO_2 has not been examined extensively.

The first report of the photo-electrochemical reduction of CO_2 was shown by Halmann in 1978.[33] The photo-reduction was carried out using p-type gallium phosphate (p-GaP) as the photocathode with part or all of the energy was supplied by light. The products were found to be formaldehyde (HCHO), formic acid (HCOOH), and methanol (CH_3OH). A presumed mechanism for the cathodic reduction of CO_2 involves a two-step electron transfer for the formation of formic acid and is as follows:

$$CO_2 + e^- \rightarrow CO_2^{\bullet-} \Leftrightarrow {}^{\bullet}HCO_2 \quad (11)$$

$${}^{\bullet}HCO_2 + e^- \rightarrow HCO_2^- \Leftrightarrow {}^{\bullet}HCOOH \quad (12)$$

Comparatively, due to high over potentials for formic acid reduction in electrochemical systems utilizing metal cathodes, the reduction essentially stops at this point. However, in the photo-electrochemical route, further reduction of formic acid occurs more readily enabling the production of other products such as formaldehyde and methanol.

Subsequently, a report by Inoue *et al.*[34] studied the photo-catalytic reduction of CO_2 with an array of semiconductors: tungsten trioxide (WO_3), titanium dioxide (TiO_2), zinc oxide (ZnO), cadmium sulfide (CdS), GaP, and silicon carbide (SiC). Their report utilized irradiation by a xenon- and mercury-lamp to produce products of HCHO, HCOOH, CH_3OH, and trace amounts of methane (CH_4) and carbon monoxide (CO). Later reports have focused on better understanding the mechanism and improving the efficiencies of such systems by examining other semiconductors and operating parameters. The literature indicates that photo-electrochemically products such as $(COOH)_2$,[44] CH_3OH,[45] HCOOH,[43] can be produced selectively, with Faradaic efficiencies of 38, 96, and 37.8%, respectively. While photo-catalytically, C_1-C_3 products have been reported;[46-49] however, the yields for photo-catalytic reduction are low and are on the order of magnitude of μmol gram-catalyst^{-1} h^{-1}. A summary of the literature in chronological order for the photo-electrochemical and photo-catalytic reduction is shown in Tables 3 and 4, respectively. The data presented in these tables illustrate typical products with either Faradaic efficiencies or yields/rates and are dependent upon many variables such as catalyst, catalyst modification, electrolyte/reductant, lamp (photon) source, temperature/pressure, which have been discussed in more detail within the literature. Although a more insightful analysis would lend

itself to examining conversion efficiencies and quantum yields, often the data are not readily available.

2.2 Concepts on the Activation of CO_2

Carbon dioxide is a colorless, odorless, and a relatively inert gas. As a linear molecule with a double bond between the carbon and oxygen atoms (O = C = O) there is no dipole moment. In nature, CO_2 serves as a carbon source for the photosynthesis of organic compounds. Natural photosynthesis in plants occurs through several steps involving dark and light reactions to generate carbohydrates and oxygen from abundant raw reactants, CO_2 and H_2O. For the case of the activation of CO_2 in dark reactions, artificial systems simulating such reactions are discussed elsewhere.[50] Over the past twenty years, a great deal of effort has been devoted to understand and mimic the mechanism of the light reactions in photosynthesis in which light energy is transformed into chemical energy. During this process, activation of CO_2 is achieved through a chain of electron carriers and chromophores. The work of Collin *et al.*[51] and Balzani *et al.*[52] cover artificial photosynthesis from the point of view of energy transfer and charge separation in multiple-component systems with transitional metal complexes. Although such homogeneous and microheterogeneous systems have shown to successfully reduce CO_2 to fuels such as formic acid,[53] methanol,[54] and methane,[55] such systems have draw backs such as low turnover numbers (mol reduced product of CO_2/mol catalyst), low yields of only single carbon products, and the lifetime along with the selectivity of single components is not well understood. Moreover, such studies focus on homogeneous metal complexes, which can be expensive and are not practical for large-scale purposes. Thus the question arises, why is it so difficult to mimic nature and is it really possible? To answer such questions, a closer examination of thermodynamics and the bonding orbitals of CO_2 are required.

Being the most abundant and oxidized form of carbon occurring in nature, it is also one of the most stable of carbon compounds. A strong indication of a CO_2 molecule's stability can thermodynamically be inferred by its large, negative standard Gibbs free energy of formation value ($\Delta_f G^{\ominus}$ = -349.67 kJ mol^{-1}).[56] Given that CO_2 is such a stable compound, consequently a substantial input of energy or a high-energy substrate is required for chemical conversion. This problem can be resolved with catalyst development; however, an important consideration for feasibility is a close examination of the thermodynamics of such reactions as shown in Table 2.

When first examining Table 2, it is noted that several of the reactions involving CO_2 are exothermic in light of the stability of the CO_2 molecule. It is worth mentioning that endothermic reactions, such as eqn 4 among several others, can be feasible and indeed useful. For example, some industrial endothermic reactions used today on large-scale are thermal cracking of hydrocarbons, dehydrogenation reaction of ethylbenzene to make styrene, and steam reforming for producing synthesis gas. Nevertheless, chemical reactions are driven by the difference in Gibbs free energy of products and reactants as shown by eqn 10. It is clear that most of the reactions in Table 2 have positive $\Delta G^{\ominus}$ values and thus are not thermodynamically favored.

$$\Delta G = \Delta H - T\Delta S \tag{10}$$

For values in Table 2 where $\Delta G^{\ominus} < 0$, they correspond to hydrogenation reaction, leading to products containing C-O, for the most part. A reason for the relatively favorable values of $\Delta G^{\ominus}$ for hydrogenation is that water is produced. However, it is important to note that these values involve the use of hydrogen. The hydrogen has to either be supplied by an outside source or via water splitting reaction in which both cases present their respective problems. For the latter case, the competition between electrons for water splitting and for CO_2 reduction arises in aqueous medium resulting in lower conversions and efficiencies. For the former case, if hydrogen is not

produced through alternative energy methods it does not favor the overall goal of CO_2 mitigation and utilization.

In the light of the results presented by this examination, thermodynamic arguments are not sufficient to explain the limited conversion of CO_2 into value added products via a technical processes. However, the reasons are kinetic in orgin. A major factor is attributed to the large energy gap between the lowest unoccuped molecular orbital (LUMO) and the highest occupied molecular orbital (HOMO) (13.78 eV)[57] as well as a large electron affinity (-0.6 ± 0.2 eV).[58] While the HOMO level is a non-bonding π orbital, this attribute makes the activation difficult since the occupation by electrons within the non-bonding HOMO levels does not change the bond order between the C-O bond and these act as a lone pair of electrons. Additional challenges of activating CO_2 molecules arise from the molecule's symmetry. Due to the charge density symmetry of the HOMO energy level, any activation will be reflected on both sides of the molecule and hence preferential conversion is not realized. These innate properties of the CO_2 molecule are on par with inert gases. Activation of such molecules has been a formidable challange within the catalyst community.

Even though several methods of activating CO_2 molecules have been proposed, as outlined in Scheme 1, a facile method to selectively activate the CO_2 molecule and convert it into useful chemicals has yet to be fully developed. Furthermore, a close examination of the bonding orbitals shows that activation of CO_2 has to be aimed at activating the carbon center in order to achieve such goals. The energies of the 2s and 2p orbitals of carbon are -19.4 and -10.7 eV while the energies of the 2s and 2p orbitals of oxygen are -32.4 and -15.9 eV, respectively.[57] This means that the 2s level of oxygen may not effectively participate in the bonding, whence the bonding levels come from the overlap of 2s and 2p orbitals of carbon with the 2p orbitals of

oxygen. Optical activation of CO_2 would require nearly 13.8 eV[59] and cannot be specific at activating the carbon center of the molecule. As direct optical activation is difficult, the activation must be realized through the removal/addition of electrons. One such avenue is the charge transfer phenomenon known in semiconductor catalysis (e.g., semiconductor photo-catalysis). Although charge transfer via semiconductor catalysis provides a simpler route for CO_2 activation, it also imposes limitations on the position of the CB of the material to facilitate smooth charge transfer from an excited semiconductor to the CO_2 molecule. Since the σ-bonding orbitals of CO_2 are deep down (-38 eV),[57] it is deduced that only the π-orbitals of CO_2 alone may be perturbed and an attack on the oxygen centers alone may be possible. Thus it may be possible to activate CO_2 molecules by charge transfer route.

The simplest reduction products that could be produced from CO_2 reduction are CO and $HCOO^-$. One, two, four, six and eight electron reduction potentials (*vs*. NHE) for CO_2 reduction and H_2O oxidation at pH 7 and 25 ^oC are given in Table 5, assuming unit activities for all gaseous and aqueous species.[60] From Table 5, it is clear that CO_2 photo-reduction is not a single-step reaction. Additionally, single electron transfer to CO_2 is energy input intensive because of the negative adiabatic electron affinity of CO_2 (*vide supra*). Upon transfer of one electron, the structure of CO_2 changes form linear to bent,[61] which results in an irreversible reduction and the formation of a negatively charged $CO_2^{\bullet -}$ species.[62,63] Therefore, the first plausible step in CO_2 photo-reduction on photoilluminated semiconductor surfaces is its activation to form $CO_2^{\bullet -}$ species. The distortion of $CO_2^{\bullet -}$ species is attributed to the repulsion among the two lone electron pairs on the oxygen atoms and the unpaired electron on the carbon atom. Consequently, the lower the O-C-O bond angle, the higher charge of the $CO_2^{\bullet -}$ moiety and the greater possibility of charge transfer to CO_2 by lowering its LUMO.

2.3 Effect of reductant on mechanism pathway

The use of water as a solvent for the photo-reduction of CO_2 is as attractive option as it is readily available and inexpensive. Two important species involved in the CO_2 photo-reduction are H• (hydrogen atom) and $CO_2^{\bullet-}$ (carbon dioxide anion radical) which are produced by electron transfer from the conduction band as seen in eqns 13 and 14:

$$H^+ + e_{CB}^- \rightarrow H^\bullet \tag{13}$$

$$CO_2 + e_{CB}^- \rightarrow CO_2^{\bullet-} \tag{14}$$

These radicals also form other stable substances. However, the solubility of CO_2 in water is low and competition with H_2 and H_2O_2 formation consumes H^+ and e_{CB}^- as:

$$photocatalyst + 4h\nu \Leftrightarrow \left(4h_{VB}^+ + 4e_{CB}^-\right) \tag{15}$$

water decomposition

$$2H_2O + 4h_{VB}^+ \rightarrow O_2 + 4H^+ \tag{16}$$

hydrogen formation

$$4H^+ + 4e_{CB}^- \rightarrow H_2 \tag{17}$$

hydrogen peroxide formation

$$O_2 + 2H^+ + 2e_{CB}^- \rightarrow H_2O_2 \tag{18}$$

As a result of these limitations, some studies have attempted to replace water with other reductants. Liu *et at.*[64] conducted experiments with solutions with various dielectric constants and concluded that low polarity solvents yield CO as the primary product. This is attributed to the $CO_2^{\bullet-}$ anion not readily dissolved and strongly adsorbed to the surface of the photo-catalyst through the carbon atom of another $CO_2^{\bullet-}$ anion. On the other hand, for higher dielectric solvents (e.g. water) the $CO_2^{\bullet-}$ anions are greatly stabilized by the solvent resulting in weak interactions

with the photo-catalyst surface. The carbon atom of the radical can react with a proton, which results in the formation of formic acid.

$$CO_2^{\bullet-} + CO_2^{\bullet-} \rightarrow CO + CO_3^{-} \quad (19)$$

$$CO_2^{\bullet-} + 2H^+ + 2e_{CB}^- \rightarrow HCOOH \quad (20)$$

A study of CO_2 photo-catalysis in the absence of a reductant was performed by Kaneco and coworkers.[65] A suspension of titania powder in supercritical CO_2 was illuminated by a Xe lamp. Following the irradiation, degassed aqueous solution was added to protonate the reaction intermediates on the titania powder. The results showed that CO_2 molecules interact with the excited-state photo-catalyst surface, resulting in the formation of $CO_2\bullet^-$ radicals. During irradiation, no gaseous reduction products were identified. It was inferred that the $CO_2\bullet^-$ anion radicals cannot be adsorbed on another $CO_2\bullet^-$ anion radical, because the excited surface of the photo-catalyst is more active than the $CO_2\bullet^-$ radical. However, following a washing process with several solvents, formic acid was detected. From these studies, it was noted that the amount of H^+ in the reductant controls the direction and selectivity of the CO_2 photo-reduction products and the amount of formic acid increased with the pH of the solution.

Improving the efficiency in aqueous systems using sacrificial electron donors such as trimethylamine, triethanolamine,[66] dimethyformamide,[67] and isopropyl alcohol[68] has also been extensively studied. Beyond the use of water as a reductant, CO_2 photo-catalysis can be achieved in the presence of gas-phase H_2S,[69] H_2,[70,71] and CH_4.[72] The use of hydrogen as an alternative for photo-catalytic reduction of CO_2 has also been investigated.[73,74] The primary products were found to be CO. Although CO may be toxic it serves as a valuable substrate for many industrial processes, such as Fischer-Tropsh synthesis or methanol synthesis. The first step in CO formation produces formate from CO_2 and H_2. The second is the reduction of CO_2 to CO on the

formate radical.

2.4 Surface state & surface site on CO_2 activation

Mechanisms presented within the literature for the photo-catalytic reduction of CO_2 indicate that CO_2 gains electrons from the CB of the photo-catalyst; however, when probed deeper, it appears not to be as straightforward. Semiconductor mediated photo-induced electron transfer reactions require the electrons in the conduction band of the semiconductor to have greater energy than that of the LUMO of the electron-accepting species. Using the values for the energy of the TiO_2 conduction band and the standard reduction potential for the HCOOH/ H_2CO_3 couple at pH = 5, for example, Xu and Schoonen[75] suggested that the electrons in the conduction band of (bulk) TiO_2 may not be transferred to CO_2. However, electronic interaction between the TiO_2 surface and CO_2 could facilitate electron transfer by lowering of the LUMO of the adsorbate by forming a surface state in the band gap. Such observations suggest that not much is known about the initial steps of CO_2 activation during photo-catalytic reduction. As a result, a better understanding of the interaction and charge transfer between the excited semiconductor surface and CO_2 is required.

Charge transfer from excited semiconductor surfaces to CO_2 is influenced by both bulk and local interactions. There are two different ways to understand electron transfer to CO_2 in semiconductor photo-catalysis: surface site and surface state. A surface site is a collection of atoms on the surface, which is reactive in some manner. These sites may be an oxygen vacancy or a coordinatively under-saturated metal atom, or a combination of features that results in an orbital containing unusual electron affinity. On the other hand, a surface state is a localized energy level at the surface. The occupation of the surface state with respect to the Fermi energy (E_f) of the solid determines its occupation.

2.4.1 Surface state CO_2 activation

To better determine the feasibility of electron transfer from the CB of a photo-catalyst to CO_2 an understanding of surface state energy levels for the CO_2/ $CO_2^{\bullet-}$ couple at the photocatlyst surface is required. A methodology to determine the energy levels of the surface state at the solid-gas interface has been proposed by Morrison.[76] Accordingly, the location of the standard redox potential with respect to the edges of the CB and VB of the solid at the point-of-zero-charge (pzc) determines the potential for electron transfer. The standard reduction potential for the CO_2/ $CO_2^{\bullet-}$ redox couple is -1.9 V,[77] which corresponds to a redox state with an energy level of -2.6 eV (in AVS). The main contributions to this energy are the electron affinity (-0.6 eV) and the solvation of $CO_2^{\bullet-}$ in water (-3.2 eV). The high free energy of solvation indicates that solvent reorganization energy will be significant. If one compares the redox couple of CO_2/ $CO_2^{\bullet-}$ with the location of the CB of titania in aqueous solution, without any specific interaction with the catalyst/electrode surface, it is clear that the reduction of CO_2 on titania is unlikely as the energy level associated with the CO_2/ $CO_2^{\bullet-}$ redox couple is higher in energy. As a result, a fluctuating energy level mechanism is required to describe energy levels of CO_2 and $CO_2^{\bullet-}$.

Surface states may be identified experimentally via spectroscopic studies of CO_2 adsorbed on well-defined surfaces. Using ultraviolet photoemission spectroscopy (UPS) and metastable impact electron spectroscopy (MIES), Krischok *et al.*[78] found that CO_2 interacted with rutile titania single crystals weakly, forming linearly adsorbed species. An *ab initio* periodic study of CO_2 adsorption on rutile titania supports these results.[79] Therefore, without irradiation, CO_2 does not form a surface state upon linear adsorption in the ground-electronic state. Once the photo-catalyst surface is irradiated with light energy greater than the band gap, electrons populate the CB. The energy of the CB electrons is likely to be less than that required for CO_2

reduction to $CO_2^{\bullet-}$. From this analysis, it is clear that the energy levels of CO_2/ $CO_2^{\bullet-}$ couple require a combination of local and collective approaches.

2.4.2 Surface site CO_2 activation

Studies of surface photo-catalytic processes has progressed from a surface state approach to a more detailed understanding of specific surface adsorbate structures, which are involved in the charge transfer. An examples such a study is by Nowotny *et al.*[80] on understanding the initial steps of H_2O oxidation on titania. As mentioned previously, the initial activation of CO_2 via a semiconductor photo-catalytic process is not well understood. Consequently, a better understanding of local chemistry at surface sites where activated species are formed is necessary to understand the nature of charge transfer from a metal oxide surface to CO_2. CO_2 can be adsorbed as a carbonate and a linear species on metal oxide surfaces. Various ground-state adsorbate configurations of CO_2 on titania surfaces have been studied.[79,81-83] When CO_2 is adsorbed on a titania surface, it acts as a net electron donor when it absorbs with the oxygen end on Ti Lewis acid sites, and a net electron acceptor when the electrophillic C atom interacts with surface Lewis basic sites, or surface O atoms.[62] The interaction between the C atom of CO_2 and the surface oxygen atoms of a metal oxide photo-catalyst causes the formation of surface carbonate and bicarbonate species. Conversely, if CO_2 does not interact strongly with the ground state of the semiconductor, the LUMO of adsorbed CO_2 may not be lowered enough to ensure electron transfer from the conduction band. Questions to be addressed by a surface site approach are:

- Upon illumination of a semiconducting surface, how does electron transfer from the conduction band to CO_2 occur?
- What specific sites and specific CO_2 configurations on the semiconductor surface

promote this electron transfer? Can such sites be engineered?

A strong interaction between the metal oxide surface and CO_2 is presumed for CO_2 to become activated from electrons from the CB of the semiconductor. For example, consider the case of a widely studied semiconductor photo-catalyst, TiO_2. Photoillumination of titania produces electron-hole (Ti^{3+}-O^-) centers in titania (eqns 1, 2, and 15). The Ti^{3+} centers are proposed to interact with CO_2 to form $CO_2^{\bullet-}$ species adsorbed on the surface. Further reactions involving these carbon dioxide radial anions go to from C radicals and CH_XO_y end products. The presence of suitable unoccupied molecular orbitals on CO_2 is required for the electron transfer from the Ti^{3+} surface electron centers to CO_2. For effective formation of desirable products, electronic interaction between the surface and CO_2 is necessary for CO_2 to gain electrons. One role of the surface might be to interact with CO_2 reducing the bond angle. Freund and Roberts indicate that the LUMO of CO_2 decreases with the O–C–O bond angle.[62] The lowering of the LUMO corresponds to the formation of carbonate species on the surface. The application of this principle is not limited to CO_2 activation on irradiated metal oxide surfaces. Similar interactions of CO_2 with electrocatalysts are supposed to decrease the overpotential for CO_2 reduction during electrochemical reduction.[84] Analytical techniques such as FTIR spectroscopy have been used to study adsorbed CO_2 on surface electron centers (Ti^{3+}) created due to oxygen vacancies.[81]

2.5 Effect of support and metal doping on CO_2 activation

The use of promoters such as potassium (K) or impregnation with metals has been used to improve photo-catalytic activity. Alkali promotion of CO_2 activation on titania has been studied.[85] The added alkali atom donates an electron to CO_2 to form $CO_2^{\bullet-}$. This then reacts with surface oxygen to from carbonate species on the surface. These promoters are stoichiometrically consumed upon charge transfer to CO_2 and cannot be regenerated. On the other hand,

modification with metals such as Pd, Rh, Pt, Cu, *etc*. can affect the thermodynamics and kinetics of CO_2 activation and further conversion and selectivity of products. Previous photo-catalytic studies have been performed on the loading of photo-catalysts with metals that function as electron sinks. Charge carrier traps suppress recombination and increase the lifetime of the separated electrons and holes. The deposition of various metals can lead to the formation of C_2 and C_3 compounds for the photo-reduction of CO_2.[47-49,86]

A study by Subrahmanyam *et al*.[46] examined the role of the support on product selectivity for the photo-catalytic reduction of CO_2 to C_1-C_3 products. CO_2 conversion to C_1–C_3 compounds over these materials was specific over $TiO_2/Pd/Al_2O_3$. This study demonstrated the role of SiO_2 acid–base material support in the product selectivity compared to Al_2O_3 supported systems. In contrast to this, a bulk Pd/TiO_2 system exhibited a very high selectivity for the production of methane from the photo-reduction of CO_2.[47] The nature of the support itself changes the selectivity to C_1 and C_2 compounds. Paul and Hoffmann[87] suggested that the lowered work function of an alkali promoted surface facilitates a high probability of electron transfer to impinge neutral CO_2 molecules. Moreover, they proved that the dimerization occurs via a radical–substrate reaction mechanism in a hydrogen deficient system. In addition, Kiwi and Morrison reported[88] an effect of lithium-doping of TiO_2 anatase. It was concluded from this study that lithium doping promotes conduction band electron transfer and enhances the photo-generation of hydrogen in water cleavage reaction. The use of Li as a dopant, for example, increases the total number of basic sites by creating a low coordinated oxygen species, which leads to an increase in the basic nature of the photo-catalyst. Selectivity towards C_1 and C_2 products over such catalysts is more specific than that of higher acidic supported based systems.[46] This suggests that though the basic nature of the support is of fundamental

importance, it is not alone responsible for controlling the selectivity during the photo-catalytic reduction of CO_2.

Several researchers have investigated the efficiency and selectivity by modifying the photo-catalyst surface with metal. In general, the performance of CO_2 photo-reduction to produce formaldehyde, methanol, and methane, which consume more electrons, is increased. This is attributed to the metal contacts on the semiconductor surface, which enables electrons to easily flow from the semiconductor to the metal and distribute on the surface. Additionally, the holes are then free to diffuse to the semiconductor surface, where oxidation of organic species can occur. The metal loading must be optimized and uniformly dispersed over the photo-catalyst. An excess metal loading results in a decreased illuminated photo-catalyst surface, as photons cannot be absorbed because of reflection. In a study of photo-induced CO_2 dissociation on titania-supported noble metals, it was found that the activity towards CO dissociation correlated with the work function of the polycrystalline metal for titania-supported Pt, Rh and Ir/TiO_2.[83] The following mechanism was proposed: Chemisorption of CO_2 on polycrystalline metal islands results in a bent $CO_2^{\bullet -}$ species formed by back donation between the metal d-orbitals and the (C–O) π^* orbitals. This electron transfer results in the depopulation of the metal surface state. Photo-generated electrons generated upon band gap illumination would be transferred from the conduction band of TiO2 to the metal island as a result of the work function of these metals being higher than that of reduced TiO_2. Additionally, the study by Rasko[83] demonstrates that an understanding of both surface states as well as surface sites is required to understand CO_2 activation on such TiO_2-supported metal photo-catalysts.

3. Concluding remarks

Though one can consider the importance of converting carbon dioxide into useful chemicals and fuels, the knowledge base that is obtainable now appears to be inadequate to fulfill this

expectation. The present article therefore dealt with the limitations that exist in the development of a suitable technology for this conversion and it is hoped that further research, which has assumed already an alarming proportion, may be able to evolve a solution in the near future.

Acknowledgment

The authors acknowledge the Department of Science and Technology, Government of India for funding the National Centre for Catalysis (NCCR) at IIT-Madras. The University of Nevada, Reno (USA) facilitated the participation of YRS.

References

(1) Melillo, J. M.; McGuire, A. D.; Kicklighter, D. W.; Moore, B.; Vorosmarty, C. J.; Schloss, A. L. *Nature* **1993**, *363*, 234-240.

(2) Schimel, D. S. *Global Change Biology* **1995**, *1*, 77-91.

(3) Xiaoding, X.; Moulijn, J. A. *Energy & Fuels* **1996**, *10*, 305-325.

(4) Etheridge, D. M.; Steele, L. P.; Langenfelds, R. L.; Francey, R. J.; Barnola, J.-M.; Morgan, V. I. *Historical CO2 record form the Law Dome DE08, DE08-2, and DSS ice cores (atmospheric CO2 concentrations, Antartic ice cores)*, Carbon Dioxide Information Center, 2008.

(5) Keeling, C. D.; Whorf, T. P. *Atomspheric CO2 records from sites in the SiO air sampleing network*, Carbon Dioxide Information Analysis Center, Oak Ridge National Labority, U.S. Department of Energy, 2005.

(6) Chaplin, R. P. S.; Wragg, A. A. *Journal of Applied Electrochemistry* **2003**, *33*, 1107-1123.

(7) Jitaru, M.; Lowy, D. A.; Toma, M.; Toma, B. C.; Oniciu, L. *Journal of Applied Electrochemistry* **1997**, *2*, 875-889.

(8) Hori, Y. K., K.; Suzuki, S. *Chemistry Letters* **1985**, *11*, 1695-1685.

(9) Russell, P. G. K., N.; Srinivasan, S.; Steinberg, M. *Journal of the Electrochemical Society* **1977**, *124*, 1329-1338.

(10) Bandi, A. *Journal of the Electrochemical Society* **1990**, *137*, 2157-2169.

(11) Bandi, A.; Kuhne, H. M. *Journal of the Electrochemical Society* **1992**, *139*, 1605-1610.

(12) Schwartz, M. C., R. L.; Kehoe, V. M.; Macduff, R. C.; Patel, J.; Sammells, A. F. *Journal of the Electrochemical Society* **1993**, *140*, 614-618.

(13) Hara, K. K., A.; Sakata, T.; Watanabe, M. *Journal of the Electrochemical Society* **1995**, *142*, L57-L59.

(14) Scibioh, M. A.; Viswanathan, B. *Photo-/photoelectro-catalytic pathways for carbon dioxide reduction*; Researh Signpost: Trivandrum, Kerala India, 2002.

(15) Becquerel, E. *C.R. Acad. Sci.* **1839**, 145-149.

(16) Garrett, C. G. B.; Brattain, W. H. *Physics Reviews* **1955**, *99*, 376.

(17) Gerischer, H. *Advances in Electrochemistry and Electrochemistry Engineering*; Interscience Publishing: New York, 1961; Vol. 1.

(18) Myamlin, V. A.; Pleskov, Y. V. *Electrochemistry of Semiconductors*; Plenum Press: New York, 1967.

(19) Fujishima, A.; Honda, K. *Nature* **1972**, *238*, 37-38.
(20) Bard, A. J. *Journal of Photochemistry* **1979**, *10*, 59-75.
(21) Rajeshwar, K.; Singh, P.; DuBow, J. *Electrochimica Acta* **1978**, *23*, 1117-1144.
(22) Kitano, M.; Matsuoka, M.; Ueshima, M.; Anpo, M. *Applied Catalysis A: General* **2007**, *325*, 1-14.
(23) Gratzel, M. *Nature* **1990**, *414*.
(24) Hoffmann, M. R.; Martin, S. T.; Choi, W.; Bahnemann, D. W. *Chemical Review* **1995**, *95*, 69-96.
(25) Ollis, D. F.; Pelizzetti, E.; Serpone, N. *Environmental Science & Technology* **1991**, *25*, 1522-1529.
(26) Kamat, P. V. *Chemical Reviews* **1993**, *93*, 267-300.
(27) Harris, C.; Kamat, P. V. *ACS Nano* **2009**, *3*, 682.
(28) Kamat, P. V.; Ebbesen, T. W.; Dimitrijevic, N. M.; Nozik, A. J. *Chemical Physics Letters* **1989**, *157*, 384-389.
(29) Zhang, J. Z.; O'Neil, R. H.; Roberti, T. W. *Journal of Physical Chemistry* **1994**, *98*, 3859-3864.
(30) Hodes, G.; Cahen, D.; Manassen, J. *Nature* **1976**, *260*, 312.
(31) Anpo, M.; Takeuchi, M. *Journal of Catalysis* **2003**, *216*, 505-516.
(32) Martyanov, I. N.; Uma, S.; Rodrigues, S.; Klabunde, K. J. *Chemical Communications* **2004**, 2476-2477.
(33) Halmann, M. *Nature* **1978**, *275*, 115-116.
(34) Inoue, T.; Fujishima, A.; Konishi, S.; Honda, K. *Nature* **1979**, *277*, 637.
(35) Canfield, D.; Frese, K. W. *Journal of the Electrochemical Society* **1983**, *130*, 1772-1773.
(36) Taniguchi, I.; Aurianblajeni, B.; Brockris, J. O. M. *Electrochimica Acta* **1984**, *29*, 923-932.
(37) Hinogami, R.; Mori, T.; Yae, S. J.; Nakato, Y. *Chemistry Letters* **1994**, 1725-1728.
(38) Hinogami, R.; Nakamura, Y.; Yae, S.; Nakato, Y. *Journal of Physical Chemistry-B* **1998**, *102*, 974-980.
(39) Bradley, M. G.; Tysak, T. *Journal of Electroanalytical Chemistry* **1982**, *135*, 153-157.
(40) Bradley, M. G.; Tysak, T.; Graves, D. J.; Vlachopoulos, N. A. *Journal of the Chemical Society-Chemical Communications* **1983**, 349-350.
(41) Liu, B.-J.; Torimoto, T.; Matsumoto, H.; Yoneyama, H. *Journal of Phototchemistry and Photobiology A: Chemistry* **1997**, *108*, 187-192.
(42) Koci, K.; Obalova, L.; Placha, D.; Lacny, Z. *Collect. Czech. Chem. Commun.* **2008**, *73*, 1192-1204.
(43) Yoneyama, H.; Sugimura, K.; Kuwabata, S. *Journal of Electroanalytical Chemistry* **1988**, *249*, 143-153.
(44) Ikeda, S.; Saito, Y.; Yoshida, M.; Hidetomo Noda; Maeda, M.; Ito, K. *Journal of Electroanalytical Chemistry* **1989**, *260*, 335.
(45) Barton, E. E.; Rampulla, D. M.; Bocarsly, A. B. *Journal of the American Chemical Society* **2008**, *130*, 6342-6344.
(46) Subrahmanyam, M.; Kaneco, S.; Alonso-Vante, N. *Applied Catalysis B: Environmental* **1999**, *23*, 169-174.

(47) Ishitarri, O.; Inoue, C.; Suzuke, Y.; Ibusuki, T. *Journal of Phototchemistry and Photobiology A: Chemistry* **1993**, *72*, 269.

(48) Watanabe, M. *Surface Science Letters* **1992**, *279*, L236-L242.

(49) Irvine, J. T. S.; Eggins, B. R.; Gimshaw, J. *Solar Energy* **1990**, *45*, 27.

(50) Walther, D.; Ruben, M.; Rau, S. *Coordination Chemistry Reviews* **1999**, *182*, 67-100.

(51) Jean-Paul Collin; Harriman, A.; Heitz, V.; Odobel, F.; Sawage, J.-P. *Journal of the American Chemical Society* **1994**, *116*, 5679-5690.

(52) Balzani, V.; Juris, A.; Venturi, M. *Chemical Reviews* **1996**, *96*, 759-833.

(53) Tsujisho, I.; Toyoda, M.; Amao, Y. *Catalysis Communications* **2006**, *7*, 173-176.

(54) Amao, Y.; Watanabe, T. *Applied Catalysis B: Environmental* **2009**, *86*, 109-113.

(55) Maidan, R.; Willner, I. *Journal of the American Chemical Society* **1986**, *108*, 8100-8101.

(56) Green, D. W.; Perry, R. H. *Perry's Chemical Engineers' Handbook*; 8th ed.; McGraw-Hill, 2008.

(57) Jean, Y.; Volatron, F. *An Introduction to Molecular Orbitals*; Oxford University Press: New York, NY USA, 1993.

(58) Compton, R. N.; Reinhardt, P. W.; Cooper, C. D. *Journal of Chemical Physics* **1975**, *63*, 3821.

(59) Kimura, K.; Katsumata, S.; Achiba, Y.; Yamazaki, T.; Iwata, S. *Handbook of HeI Photoelectron Spectra of Fundamental Organic Compounds*; Japan Scientific Society Press: Tokyo, 1981.

(60) Aresta, M.; Dibenedetto, A. *Catalysis Today* **2004**, *98*, 455.

(61) Jordan, K. D. *Journal of Physical Chemistry* **1984**, *88*, 2459-2465.

(62) Freund, H.-J.; Roberts, M. W. *Surface Science Reports* **1996**, *25*, 225-273.

(63) Rasko, J.; Solymosi, F. *Journal of Physical Chemistry* **1994**, *98*, 7147-7152.

(64) Liu, B.-J.; Torimoto, T.; Matsumoto, H.; Yoneyama, H. *Journal of Phototchemistry and Photobiology A: Chemistry* **1998**, *108*, 187-192.

(65) Kaneco, S.; Kurimoto, H.; Shimizu, Y.; Ohta, K.; Mizuno, T. *Energy* **1999**, *24*, 21.

(66) Johne, P.; Kisch, H. *Journal of Phototchemistry and Photobiology A: Chemistry* **1997**, *111*, 223.

(67) Fujiwara, H.; Hosokawa, H.; Murakoshi, K.; Wada, Y.; Yanagida, S. *Journal of Physical Chemistry-B* **1997**, *101*, 8270.

(68) Kaneco, S.; Shimizu, Y.; Ohta, K.; Mizuno, T. *Journal of Phototchemistry and Photobiology A: Chemistry* **1998**, *115*, 223.

(69) Aliwi, S. M.; Aljubori, K. F. *Solar Energy Materials* **1989**, *18*, 223.

(70) Kohno, Y.; Tanaka, T.; Funabiki, T.; Yoshida, S. *Chemical Communications* **1997**, 841.

(71) Kohno, Y.; Tanaka, T.; Funabiki, T.; Yoshida, S. *Physical Chemistry Chemical Physics* **2000**, *2*, 2635.

(72) Kohno, Y.; Tanaka, T.; Funabiki, T.; Yoshida, S. *Physical Chemistry Chemical Physics* **2000**, *2*, 5302.

(73) Lo, C.-C.; Hung, C.-H.; Yuan, C.-S.; Wua, J.-F. *Solar Energy Materials and Solar Cells* **2007**, *91*, 1765-1774.

(74) Kohno, Y.; Ishikawa, H.; Tanaka, T.; Funabiki, T.; Yoshida, S. *Physical Chemistry Chemical Physics* **2001**, *3*, 1108-1113.
(75) Xu, Y.; Schoonen, M. A. A. *American Mineralogist* **2000**, *85*, 543.
(76) Morrison, R. S. *The Chemical Physics of Surfaces*, 1990.
(77) Koppenol, W. H.; Rush, J. D. *Journal of Physical Chemistry* **1987**, *91*, 4429.
(78) Kirschok, S.; Hofft, O.; Kempter, V. *Surface Science* **1982**, *507-510*, 69-73.
(79) Markovits, A.; Fahmi, A.; Minot, C. *Journal of Molecular Structure: THEOCHEM* **1996**, *371*, 219-235.
(80) Nowotny, J.; Bak, T.; Nowotny, M. K.; Sheppard, L. R. *International Journal of Hydrogen Energy* **2007**, *32*, 2651-2659.
(81) Busca, G.; Lorenzelli, V. *Journal of Materials Chemistry* **1982**, *7*, 89-126.
(82) Ramis, G.; Busca, G.; Lorenzelli, V. *Materials Chemistry and Physics* **1991**, *29*, 425.
(83) Rasko, J. *Catalysis Letters* **1998**, *56*, 11-15.
(84) Schmidt, M. In *Carbon dioxide chemistry: Environmental issues*; Paul, J. P., Claire-Marie, Eds.; RSC: Cambridge, 1994.
(85) Brause, M.; Kempter, V. *Surface Science* **2001**, *476*, 78.
(86) Khan, M. M. T.; Chatterjie, D.; Bhatt, J. *Proceedings of the Indian Academy of Sciences-Chemical Sciences* **1992**, *104*, 747.
(87) Paul, J.; Hoffmann, F. M. *Catalysis Letters* **1988**, *1*, 445.
(88) Kiwi, J.; Morrison, C. *Journal of Physical Chemistry* **1984**, *88*, 6146.
(89) Marland, G.; Boden, T. A.; Andres, R. J. *Global, Regional, and National CO2 Emissions*, Carbon Dioxide Information Analysis Center, Oak Ridge National Laboratory, U.S. Department of Energy, 2005.
(90) Song, C. *Catalysis Today* **2006**, *115*, 2-32.
(91) Zafrir, M.; Ulman, M.; Zuckerman, Y.; Halmann, M. *Journal of Electroanalytical Chemistry* **1983**, *159*, 373.
(92) Bockris, J. O. M.; Waas, J. C. *Journal of the Electrochemical Society* **1989**, *136*, 2521.
(93) Kaneco, S.; Katsumata, H.; Suzuki, T.; Ohta, K. *Chemical Engineering Journal* **2006**, *116*, 227-231.
(94) Halmann, M.; Ulman, M.; Aurian-Blajeni, B. *Solar Energy* **1983**, *31*, 429-431.
(95) Cook, R. L.; MacDuff, R. C.; Sammells, A. F. *Journal of the Electrochemical Society* **1988**, *135*, 3069-3070.
(96) Anpo, M.; Chiba, K. *Journal of Molecular Catalysis* **1992**, *74*, 207-212.
(97) Adachi, K.; Ohta, K.; Mizuno, T. *Solar Energy* **1994**, *53*, 187-190.
(98) Liu, B.-J.; Torimoto, T.; Yoneyama, H. *Journal of Phototchemistry and Photobiology A: Chemistry* **1998**, *113*, 93-97.
(99) Tseng, I.-H.; Chang, W.-C.; Wu, J. C. S. *Applied Catalysis B: Environmental* **2002**, 37-48.
(100) Guan, G.; Kida, T.; Yoshida, A. *Applied Catalysis B: Environmental* **2003**, *41*, 387-396.
(101) Pan, P.-W.; Chen, Y.-W. *Catalysis Communications* **2007**, *8*, 1546-1549.
(102) Ozcan, O.; Yukruk, F.; Akkaya, E. U.; Uner, D. *Applied Catalysis B: Environmental* **2007**, *71*, 291-297.

(103) Li, G.; Ciston, S.; Saponjic, Z. V.; Chen, L.; Dimitrijevic, N. M.; Rajh, T.; Gray, K. A. *Journal of Catalysis* **2008**, *253*, 105-110.

(104) Nguyen, T.-V.; Wu, J. C. S.; Chiou, C.-H. *Catalysis Communications* **2008**, *9*, 2073-2076.

(105) Varghese, O. K.; Paulose, M.; LaTempa, T. J.; Grimes, C. A. *Nano Letters* **2009**, *9*, 731-737.

Tables & Figures

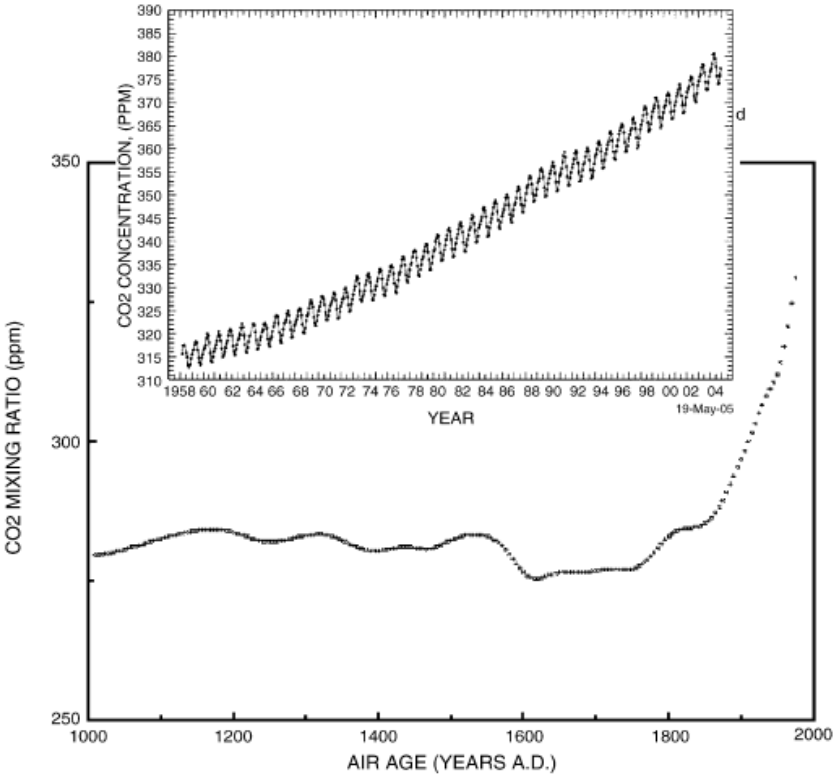

Figure 1: Atmospheric carbon dioxide (CO_2) concentrations during 1000-2004 based on the analysis of Antarctic ice cores[4] and the actual atmospheric CO_2 analysis during 1958-2004.[5]

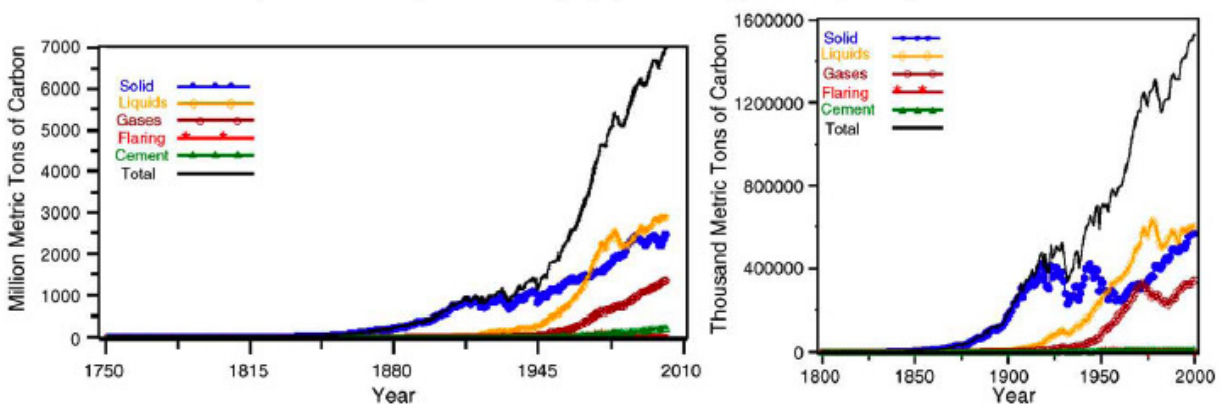

Figure 2: World carbon dioxide (CO_2) emissions in million metric tons of carbon (left) and US CO_2 emissions in thousand metric tons of carbon by fuel type (right). Taken from Marland *et al.*[89]

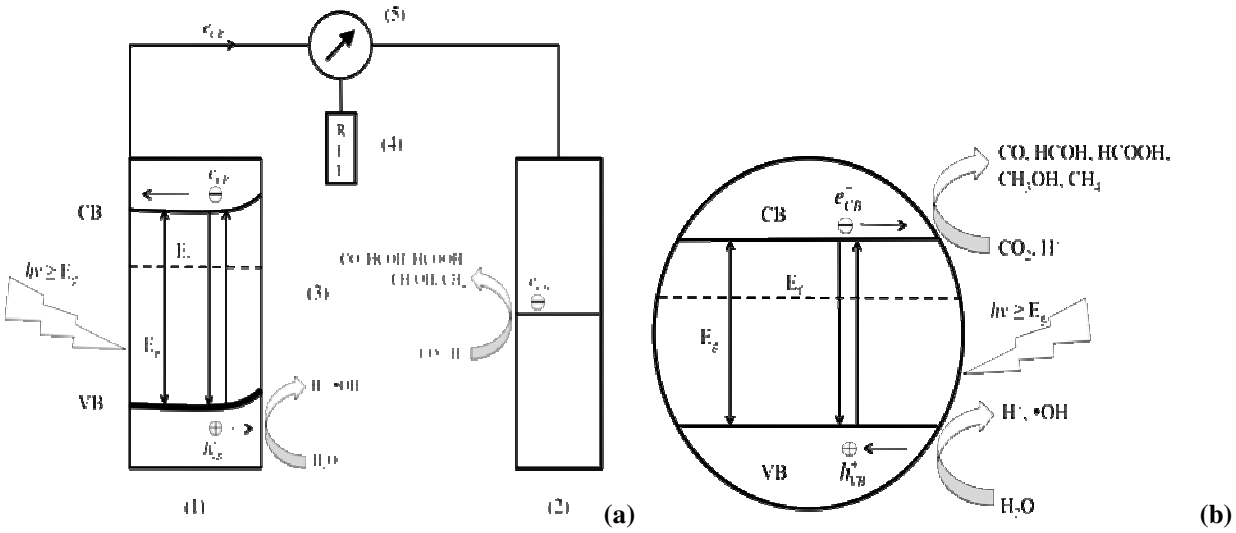

Figure 3: (a) Schematic of a liquid junction photo-electrochemical cell for a p-type semiconductor for the reduction of carbon dioxide to various products. A similar setup is used for n-type cells as well. The anode (1) is the photoactive material, (2) is the cathode, (3) a conducting electrolyte, (4) reference electrode, (5) potentiostat. In photo-catalysis a semiconductor itself can act as a photo-electrochemical cell as shown by **Figure 3b**. The valance band and conduction band of the semiconductor are analogous to the anode and cathode in a photo-electrochemical cell, respectively. The Fermi level is denoted by E_f, which is defined as the energy level in which 50% of the distribution of charge carries can be found defined by the Fermi-Dirac function.

Table 1: Sources of carbon dioxide emissions (CO_2). Taken from C. Song 2006.[90]

Stationary sources	Mobile sources	Natural sources
Fossil fuel-based electrical power plants	Cars, and sport utility vehicles	Humans
Independent power producers	Trucks and buses	Animals
Manufacturing plants in industry [a]	Aircrafts	Plants and animal decay
Commercial residential buildings	Trains and ships	Land emission leakage
Flares of gas at field	Construction vehicles	Volcanoes
Military and government facilities	Military and government devices	Earthquakes

[a] Major concentrated CO_2 sources include plants for manufacturing hydrogen, ammonia, cement, limestone, and soda ash as well as fermentation processes and chemical oxidation processed.

Table 2: Thermodynamics for various reactions involving CO_2.[62]

Reaction	$\Delta H^{\ominus}$ (kJ mol^{-1})	$\Delta G^{\ominus}$ (kJ mol^{-1})	eqn
$CO_{2(g)} + H_{2(g)} \rightarrow CO_{(g)} + H_2O_{(g)}$	41.2	18.6	(3)
$CO_{2(g)} + H_{2(g)} \rightarrow CO_{(g)} + H_2O_{(l)}$	-2.8	20.0	(4)
$CO_{2(g)} + H_{2(g)} \rightarrow HCOOH_{(l)}$	-31.2	33.0	(5)
$CO_{2(g)} + 2H_{2(g)} \rightarrow CHOH_{(l)} + H_2O_{(l)}$	-9.0	44.0	(6)
$CO_{2(g)} + 3H_{2(g)} \rightarrow CH_3OH_{(l)} + H_2O_{(l)}$	-131.3	-9.2	(7)
$CO_{2(g)} + 4H_{2(g)} \rightarrow CH_{4(g)} + 2H_2O_{(l)}$	-252.9	-130.8	(8)
$2CO_{2(g)} + 6H_{2(g)} \rightarrow CH_3OCH_{3(l)} + 3H_2O_{(l)}$	-264.9	-38.0	(9)

Table 3: Summary of the Photo-electrochemical reduction of CO_2

Catalyst(s)	Electrolyte/Reductant	Light Source	(-)E/V (SCE)	i/mA cm^{-2}	Primary Products (Faradic efficiency, %)	Notes	Reference
p-GaP	Aqueous buffer	315-510 nm	1.0	6.0	HCHO (5.6), CH_3OH (3.6)	Electrode etched in conc. HNO_3:HF:H_2O (3:1:4 v/v)	Halmann, 1978[33]
p-GaAs p-InP n-GaAs (dark)	0.2 M Na_2SO_4	W-halogen lamp	1.3	0.09, 0.06, 0.180	CH_3OH(55), (70), (100)	Electrodes etched in 1vol% Br_2/CH_3OH (v:v) in 0.1M EDTA	Canfield & Frese, 1983[35]
p-GaAs	3.1 M $CaCl_2$ + 0.87 M HCl + 0.07 M V(II)Cl_2	150 W W or XO lamp	0.7	0.85	HCOOH (1.5), HCHO (0.3), CH_3OH (0.14)	Elelctrode eteched in 5% Br_2 in CH_3OH + H_2SO_4, 30% H_2O_2 (1:1 v/v)	Zafrir *et al.* 1983[91]
p-CdTe	TBAP in DMF NH_4ClO_4 in DMF + H_2O	Xe lamp, λ = 600 nm	1.6	1.25	CO, H_2: (62.5, 0.25), (5-80%,-), increases as [H_2O] increases	CdTe electrode was best performing over several others tested, etched in aqua regia	Taniguchi *et al.* 1984[36]
	p-CdTe 0.1 M Na_2CO_3 0.1 M Li_2CO_3 0.1 M K_2CO_3 0.1 M Na_2SO_4 0.1 M K_2SO_4 0.1 M Na_3PO4 0.1 M Na_2HPO_4 0.1 M $LiClO_4$ 0.1 M TEAP				p-CdTe H_2, CO, HCOOH (40.3, 15.6, 41.8) (47.2, 10.7, 37.8) (39.7, 19.1, 35.5) (45.1, 43.3, 5.4) (51.5, 32.7, 3.4) (56.1, 25.4, 2.6) (57.2, 27.2, 1.7) (41.5, 40.5, 18.9) (10.9, 60.7, 23.8)		
p-CdTe p-InP	p-InP 0.1 M Na_2CO_3 0.1 M Na_2SO_4 0.1 M Na_3PO_4 0.1 M $LiClO_4$ 0.1 M TEAP	500 W Xe lamp (λ ≥ 450 nm)	1.24	-	p-InP (71.0, 8.6, 17.5) (70.7, 16.1, 4.6) (80.3, 10.7, 2.3) (61.8, 13.7, 24.2) (30.0, 26.0, 36.2)	p-CdTe electrode etched in $HCl+HNO_3$ (3:1 v/v) and p-InP electrode etched in 1% bromide dissolved in methanol	Yoneyama, *et al.* 1988[43]

					CO, CH_3OH, H_2		
p-CdTe bare					(92, -, 10)		
p-CdTe & 24-crown-8					(87, 6, 6)		
p-CdTe & 18-crown-6					(85, 13, 1)		
p-CdTe & 15-crown-6	0.1 M TEAP and DMF + 5%	560 nm			(-,-,94)	Electrodes etched in	Bockris & Waas,
p-CdTe & 12-crown-4	H_2O (pH = 9)	(0.5 mW cm^{-2})	1.7	-	(88, 5, 4)	aqua regia	1989[92]
					$(COOH)_2$, HCOOH, CO, H_2		
Au/p-GaP					(8, 6, 94, trace)		
In/p-GaP					(0.4, 7, 94, trace)		
Pb/p-GaP	0.1 M TEAP in				(38, 11, 41, trace)	Electrodes etched in	
Zn/p-GaP	phthalocyanine	300 W Xe lamp	1.24	-	(1, 8, 100, trace)	aqua regia	Ikeda *et al.* 1989[44]
					H_2, CO, HCOOH, CH_4		
p-Si			1.27	2.40	(73.5, 12, 4.3, 0.44)	electrodes etched in CP-	
Ag			1.49	1.69	(14.1, 75.9, 2.1, 0)	4A and 12%HF, pure	
Ag/p-Si			1.05	2.29	(38.4, 50.9, 0.8, 0)	metal electrodes	
Au			1.21	2.13	(3.7, 82.2, 0, 24, 0)	electrochemically	Hinogami *et al.*
Au/p-Si	0.1 M $KHCO_3$	W-halogen lamp	0.74	1.87	(9, 62.2, 0, 0)	polished in acid	1998[38]
					CO, HCOOH, H_2		
Pb/p-InP				Pb (5.5)	Pb (10, 30, 5)		
Ag/p-InP				Ag (10)	Ag (80, 2.5, 5)		
Au/p-InP				Au (11)	Au (70, 5, 10)		
Pd/p-InP				Pd (5.9)	Pd (45, 0, 20)	electrodes etched in CP-	
Cu/p-InP				Cu (3.8)	Cu (35, 18, 22)	4A and a mixture of	Kaneco *et al.*
Ni/p-InP	3 mM LiOH/CH_3OH	500 W Xe lamp	2.54	Ni (5.9)	Ni (12, 18, 22)	conc. Acids	2006[93]
			465 nm	465 nm	CH_3OH 465 nm		
			0.7	1.1	56		
			0.6	1.0	51		
			0.5	0.46	78		
			0.4	0.33	83		
			0.3	0.27	90		
			365 nm	365 nm	365 nm		
			0.5	0.92	62	electrode eteched in	
			0.4	0.48	89	HNO_3:HCl (2:1 v/v),	
			0.3	0.28	92	selectivity for	
		200 W W-halogen	0.2	0.21	96	methaanol favored only	Barton *et al.*
p-GaP (111)	0.5 M KCl + 10 mM pyridine	lamp	0.25	0.21	96	with pyridine	2007[45]

Table 4: Summary of the Photo-catalytic reduction of CO_2

Catalyst(s)	Electrolyte/ Reductant	Light Source	Experimental Conditions	System	Primary Products (yield/rate)	Notes	Reference
TiO_2 $SrTiO_3$ $CaTiO_3$	H_2O + $LiHCO_3$	Sunlight	Temperature and solar flux variation based on ambient conditions	1 X 0.5 m^2 solar collector, immoblized particulate films	HCOOH (10.2-518.8 μmol kJ^{-1}) HCHO (0.2-15.4) CH_3OH (2.7-48.1) CH_3CHO (0-15.4) C_2H_5OH (0-2)	South facing solar collector, natural light, conditions varied such as catalyst and electrolyte, most efficient system was $SrTiO_3$ with $LiHCO_3$	Halmann *et al.* 1983[94]
Cu/SiC	0.5 M $KHCO_3$	Hg lamp (7 mW/cm^2, λ = 365 nm)	Temperature: 273-353 K pH: 3-9	35 mL batch slurry reactor	CH_4 (14.9 μL h^{-1} g^{-1}) C_2H_4 (3.9) C_2H_6 (2.3)	Only gaseous products analyzed, selectivity toward C_2 hydrocarbon favored with Cu addition	Cook *et al.* 1988[95]
ZnO	H_2O	75 W Xe lamp (λ > 398 nm)	Temperature: 278 K Pressure: 0.25-0.35 MPa	slurry reactor	CH_3OH and CH_4		Watanabe 1992[48]
TiO_2	H_2O	75 W Hg lamp (λ > 280 nm)	Temperature: 273-323 K	particulate films, fine particle slurry, and single crystal	CH_4, CH_3OH, CO, and C_2 hydrocarbons found in trace	Product yields highly depend upon catalyst crystalline, CO_2/H_2O ratio and temperature	Anpo *et al.* 1992[96]
Cu/TiO_2	H_2O	400 W Xe lamp	ambient temperature P = 2.7 MPa pH = 5.45	42.5 mL stainless steel slurry reactor with quartz window	CH_4 (21.8 μL g^{-1}) C_2H_4 (26.2) C_2H_6 (2.7)	Product yields found to be a function of Cu loading and illumination time, 5wt.% Cu optimal	Adachi *et al.* 1994[97]
surface modified CdS with thiol compounds	2-propanol with various solvents	500 W Hg lamp (λ > 300 nm)	Ambient temperature & pressure	7 mL quartz slurry reactor	formate and CO	Dielectric constant of solvent plays a role on naked CdS toward CO selectivity	Liu *et al.* 1998[98]
$TiO_2/Pd/Al_2O_3$ $TiO_2/Pd/SiO_2$ Cu/ZnO Li_2O/TiO_2 over MgO, Al_2O_3	H_2O	250 mW Hg arc lamp	Ambient temperature & pressure	slurry reactor	CH_3COCH_3 CH_3CH_2OH CH_3OH HCOOH HCHO CH_4 C_2H_6	Selectivity for C_3 favored by $TiO_2/Pd/Al_2O_3$, basic catalyst support favored C_1-C_3 while acidic support favored C_1	Subrahmanyam *et al.* 1999[46]
Sol-gel $Cu(I)/TiO_2$	0.2 M NaOH	8 W Hg lamp, λ = 254nm	Temperature: 323 K Pressure: 0.1 MPa	300 mL slurry reactor	CH_3OH (19.7 μmol h^{-1} g^{-1})	Selectivity increased towards CH_3OH over CH_4 with Cu(I) loading	Tseng *et al.* 2002[99]
$Pt/K_2Ti_6O_{13}$ with Fe-Cu-K/DAY Zeolite catalyst	H_2O	Concentrated sunlight	Temperature: 590 K Pressure: 0.2 MPa	173 mL fixed bed	H_2 (6.17 μmol h^{-1}) CH_4 (0.014) CH_3OH (1.45) HCOOH (3.88) C_2H_5OH (0.35)	Product rates and yields found to be a function of reaction temperature and Fe:$K_2Ti_6O_{13}$ ratio	Guan *et al.* 2003[100]

TiO_2-ZrO_2	$H_2 + H_2O$	(4) 15 W UV lamps, λ = 265 and 354 nm	Temperature: 316 ± 2 K Pressure: 0.11 MPa	Gas-solid, 120 mL annular reactor, TiO_2 & ZrO_2 immobilized on pyrex glass pellets	CH_4 (8.21 μmol g^{-1}) CO (0.28) C_2H_6 (0.20)	Most effective system was TiO2 with H2+H2O, use of ZrO_2 leads to only CO productss	Lo *et al.* 2007[73]
$NiO/InTaO_4$-R50-O200	0.2 M KHO_3	500 W halogen lamp	Ambient temperature & pressure	75 mL slurry reactor	CH_3OH (1.39 μmol h^{-1} g^{-1})	Methanol rate increased with NiO loading and with R50-O200 treatment, quantum/energy efficiency of 2.54% reported for optimal system	Pan *et el.* 2007[101]
Dye $[Ru(Bpy)_3]^{2+}$, BrGly, BrAsp, sensitized, Pt-promoted, TiO_2 films	H_2O	150 W UVA and 75 W daylight lamps	Temperature: 298 K pCO_2 = 0.09 MPa	Gas-solid, glass chamber	CH_4 only monitored	Higher yields for Pt impregnated TiO2 over sol-gel Pt-TiO2 in UV, sensitizers reduced activity under UV irradiation and CH4 was observed under visible light	Ozcan *et al.* 2007[102]
Mixed phase TiO_2 powders from $TiCl_4$ hydrolysis	$NaHCO_3$ + isoporpanol	450 W medium-pressure Hg lamp, UV+vis components	Temperature: 293-298 K	1280 mL annular glass reactor	CH_4 (33.3 μmol h^{-1} g^{-1})	Anatase-rutile nanocomposite exhibited higher evolution of CH4 of commercial TiO2	Li *et al.* 2008[103]
N3-dye sensitized/ Cu(0.5wt%) /Fe(0.5wt%)/TiO_2	H_2O	Concentrated sunlight at ~25 mW cm^{-2} and artifical light at 225 mW cm^{-2} (320-500 nm)	Temperature: 348 K	216 mL, continuous circulating optical fiber reactor	Artifical light: C_2H_4 (0.562 μmol h^{-1} g^{-1}) CH_4 (0.847) Natural sunlight: CH_4 (0.617)	Higher methane rate noted for system without N3 dye under artifical light conditions where as ethlyene remains faily constant, no ethylene detected under natural concentrated light	Nguyen *et al.* 2008[104]
Nitrogen doped nanotublar films of Pt/TiO_2 Cu/TiO_2	H_2O	Sunlight, measured between 75-102 mW cm^{-2}	Temperature: 317 ± 4 K Pressure: 0.11 MPa	Gas-solid, 7.5 and 8.6 mL stainless steel reactor with quartz window	H_2, CO, CH_4, other alkanes, olfin, and branched paraffin, hydrocarbon rate ~160 μL h^{-1} g^{-1}	Nanotube length, crystalline, and cocatalyst play a role in the production rates hydrocarbons, Pt cocatalyst plays a role in H_2/CO selectivity	Varghese *et al.* 2009[105]

Table 5: Reduction potentials (*vs.* NHE) of some reactions involved in CO_2 reduction at pH = 7 and unit activity.

Reaction	E^o, V (*vs.* NHE)
$2H^+ + 2e^- \rightarrow H_2$	-0.41
$H_2O + ½\ O_2 + 2H^+ + 2e^-$	0.82
$CO_2 + e^- \rightarrow CO_2^{\bullet -}$	-1.90
$CO_2 + H^+ + e^- \rightarrow HCO_2^- + H_2O$	-0.49
$CO_2 + 2H^+ + 2e^- \rightarrow CO + H_2O$	-0.53
$CO_2 + 4H^+ + 4e^- \rightarrow HCHO + H_2O$	-0.48
$CO_2 + 6H^+ + 6e^- \rightarrow CH_3OH + H_2O$	-0.38
$CO_2 + 8H^+ + 8e^- \rightarrow CH_4 + 2H_2O$	-0.24

Scheme 1: Various modes of activating CO_2

Radiochemical

$$CO_2 \xrightarrow{\gamma - radiation} HCOOH, HCHO$$

Chemical reduction

$$2Mg^{2+} + CO_2 \longrightarrow 2MgO + C$$
$$Sn^{4+} + 2CO_2 \longrightarrow SnO_2 + 2CO$$
$$2Na^{+} + 2CO_2 \longrightarrow Na_2C_2O_4$$

Thermo chemical

$$CO_2 \xrightarrow{Ce^{4+} + h\nu} CO + \tfrac{1}{2} O_2 \ (T > 900^{o}C)$$

Photochemical

$$CO_2 \xrightarrow{h\nu} CO, HCHO, HCOOH$$

Electrochemical

$$CO_2 + xe^{-} + xH^{+} \longrightarrow CO, HCOOH, (COOH)_2$$

Biochemical

$$CO_2 + 4H_2 \xrightarrow{bacteria} CH_4 + 2H_2O$$

Photo-electrochemical

$$CO_2 + 2e^{-} + 2H^{+} \xrightarrow{h\nu} CO + H_2O$$

Bioelectrochemical

$$CO_2 + \text{oxoglutaric acid} \xrightarrow{enzyme + methylvio\log en} \text{isocitric acid}$$

Biophtotoelectrochemical

$$CO_2 \xrightarrow{h\nu + enzyme + methlyvio\log en + p-\ln P} HCOOH$$